Western diet enhances intestinal tumorigenesis in *Min* mice, associating with mucosal metabolic and inflammatory stress and loss of *Apc* heterozygosity

M Niku [1,2], A-M Pajari[1], L Sarantaus[3], E Päivärinta[1], M Storvik[4], A Heiman-Lindh[1], M Nyström[3], M Mutanen[1]

[1] Department of Food and Environmental Sciences, Division of Nutrition, P.O. Box 66 (Agnes Sjöbergin katu 2), FI-00014 University of Helsinki, Finland;

[2] Current address: Department of Veterinary Biosciences, P.O. Box 66 (Agnes Sjöbergin katu 2), FI-00014 University of Helsinki, Finland

[3] Department of Biosciences, P.O. Box 65, FI-00014 University of Helsinki, Finland

[4] School of Pharmacy, University of Eastern Finland, P.O. Box 1627, FI-70211 Kuopio, Finland

M Niku and A-M Pajari share the first authorship of this article

Running Title:

Western-type diet accelerates tumorigenesis in *Apc*$^{Min/+}$ mice

Keywords:

High-risk Western-type diet, PDK4, ERK, energy metabolism, *Apc*$^{Min/+}$ mice

Grant Support:

This work was supported in part by European Research Council (2008-AdG-232635), Albin Johansson and Yrjö Jahnsson foundations.

Corresponding author

M Mutanen, P.O. Box 66 (Agnes Sjöbergin katu 2), FI-00014 University of Helsinki, Finland

Tel.: +358504151612, Fax : +358 9 19158269, e-mail: marja.mutanen@Helsinki.fi

Disclosure of Potential Conflicts of Interest

The authors disclose no potential conflicts of interest.

Authors' Contributions

Conception and design: Mutanen, Nyström, Päivärinta, Niku

Acquisition of data (provided animals, feeding and operation of animals, laboratory analyses): Päivärinta, Niku, Sarantaus, Heiman-Lindh,

Analyses and interpretation of the data: Storvik, Mutanen, Niku, Pajari, Päivärinta

Writing, review and/or revision of the manuscript: Mutanen, Niku, Pajari, Storvik

Study supervision: Mutanen, Nyström, Pajari

Word count: 4895

Total number of figures and tables: 7

Abstract

Western-type diet (WD) is a risk factor for colorectal cancer but the underlying mechanisms are poorly understood. We investigated the interaction of WD and heterozygous mutation in the *Apc* gene on adenoma formation and metabolic and immunological changes in the histologically normal mucosa of $Apc^{Min/+}$ (*Min/+*) mice. The diet used was high in saturated fat and low in calcium, vitamin D, fiber and folate. The number of adenomas was twofold higher in the WD mice compared to controls, but adenoma size, proliferation or apoptosis did not differ. The ratio of the *Min* to wild-type allele was higher in the WD mice, indicating accelerated loss of *Apc* heterozygosity (LOH). Densities of intraepithelial $CD3\varepsilon^+$ T lymphocytes and of mucosal $FoxP3^+$ regulatory T cells were higher in the WD mice, implying inflammatory changes. Western blot analyses from the mucosa of the WD mice showed suppressed activation of the ERK and AKT pathways and a reduced activation of the mTOR pathway as measured in phosphoS6/S6 levels. The expression of pyruvate dehydrogenase kinase 4 (PDK4) was strongly upregulated in both mRNA and protein levels. Microarray analyses showed changes in oxidation/reduction, fatty acid, and monosaccharide metabolic pathways, tissue organization, cell fate and regulation of apoptosis. Together, our results suggest that the high-risk Western diet primes the intestinal epithelium to tumorigenesis by programming a cancer-type energy metabolism, and by inducing metabolic and inflammatory oxidative stress, which accelerate LOH of the *Apc* gene.

Introduction

Colorectal cancer (CRC) is one of the most common cancer types in industrialized countries. An inactive lifestyle, obesity, and a high-fat diet with low micronutrient density are well-known risk factors for CRC, and studies in various animal models support the role of a high-

risk Western-type diet, i.e. a diet that is high in fat and low in fiber, calcium, vitamin D and folate, in colon tumorigenesis (1-4). Mechanisms for how the unbalanced, high-energy yielding Western-type diet predisposes or promotes the intestinal epithelium to carcinogenesis are poorly understood.

Components of the Wnt signaling pathway are almost ubiquitously mutated in CRC, most typically the *Apc* gene, and mutations in the *APC* gene are found in the majority of sporadic CRC cases (5). APC regulates β-catenin pools in cells. Increased nuclear accumulation of β-catenin is one of the driving forces for colon tumorigenesis (6).

Recent research connects the activation of Wnt signaling with dysregulation of energy metabolism so that its activation drives increased use of glucose, i.e. Warburg-type cancer metabolism (7). Increased glycolytic rate in transformed cells elevates the production of glycolytic intermediates, which are used in the biosynthetic pathways to satisfy the anabolic needs of dividing cells (8). This provides a selective growth advantage for transformed cells. Furthermore, mitochondrial metabolism is shifted to uncoupled oxidation of glutamine and fatty acids to maintain glycolysis. These alterations in cellular metabolism predispose cells to an increased load of reactive oxygen species that activate apoptosis or, if the cell does not undergo apoptosis, may induce tumorigenic proliferation and anchorage-independent growth (9). Earlier it was believed that the Warburg effect is secondary to transformation, but the metabolic changes seem to occur already during the transformation process and are governed by the same signal transduction pathways as proliferation (10). Interestingly, an earlier study (4) demonstrated that a Western-type diet reprograms the intestinal

epithelium towards a gene expression pattern resembling that driven by *Apc* mutations. Thus, dietary and genetic factors converge in driving intestinal tumorigenesis.

In the glycolytic switch, pyruvate dehydrogenase kinases (PDKs) act as key regulators. These inactivate the pyruvate dehydrogenase complex, which catalyzes the rate-limiting step for channeling pyruvate into the tricarboxylic acid cycle. Increased PDK4 expression has been reported in preneoplastic intestinal epithelium of cancer-susceptible mice and CRC patients. In addition, it is known that PDK inhibition can suppress tumor growth (11, 12). On the other hand, many tumors show lower PDK4 expression in comparison to the normal tissue of origin, indicating that the metabolic demands in the various stages of carcinogenesis are different (13). PDK4 expression is negatively regulated by the PI3 kinase/AKT and ERK1/2 pathways, which control nutrient uptake and convey growth factor signals to the mTOR kinase, promoting cellular growth and differentiation (13, 14). These pathways are commonly overactivated in CRC and other cancers (15, 16).

We have earlier shown that high fat content in an otherwise balanced diet does not promote intestinal tumorigenesis in the *Apc* –mutated *Min/+* mouse (17), a widely used murine model of human intestinal carcinogenesis. Here we have further studied tumor formation in the *Min/+* mouse by combining the high fat content with marginal concentrations of fiber, calcium, vitamin D and folate to better mimic a typical Western-type diet. Several of these components have been shown to interact with β-catenin metabolism (18-20).

We found that the high-risk Western-type diet accelerated adenoma formation, but not growth, in the *Min/+* mouse. Increases in adenoma numbers were accompanied by loss of heterozygosity (LOH) in the *Apc* gene, downregulation of ERK1/2, AKT and mTORC1 signalling pathways, as well as changes in the density of immune cells in the normal appearing mucosa of the *Min/+* mouse. Microarray analyses showed several changes in the key cellular pathways regulating energy metabolism, tissue organization and cell fate, all of which could predispose the intestinal epithelium to enhanced tumorigenesis.

Materials and Methods

Animals and diets

Male and female C57BL/6J *Min/+* mice were bred at the Laboratory Animal Centre in Viikki, Helsinki, from inbred mice originally obtained from the Jackson Laboratory (Bar Harbor, ME, USA). After weaning, the mice were PCR screened for the *Min*/+ genotype. The 5-week old *Min/+* mice were stratified by weight and litter background and assigned into experimental diets. The mice were housed in plastic cages in humidity- and temperature-controlled facilities with a 12-h light-dark cycle. They were fed *ad libitum* and had free access to tap water. The mice were weighed and monitored weekly and a record was kept on their growth throughout the experiment. One mouse from the WD group had to be sacrificed before the end of the experiment due to considerable weight-loss during one week and was consequently excluded from the subsequent analyses. The total number of mice included in the data was 12 in the WD diet group and 14 in the control diet group. The control diet was the semisynthetic unmodified AIN-93G diet. The WD was modified from AIN-93G, with high fat and low fiber, vitamin D, calcium and folate (Table I; Harlan Teklad, Madison, WI). We

used our own modification of the Western-type diet, which highly resembles the New Western Diet (NWD) used by Newmark et al (2). shown to induce benign and malignant neoplasms in the colon of normal B6 mice after an 18 month feeding experiment The main difference between NWD and our WD is the source of fat, which in our diet resembled the more typical consumption of fat in Western populations, and was largely composed of milk fat (66.4% of total fat from milk, and 33.6% from rapeseed and sunflower oil) while in the NWD the main fat source was corn oil. The Laboratory Animal Ethics Committee, University of Helsinki approved the study protocol.

Evaluation of adenomas and collection of samples

After the 10-week feeding period, the mice were sacrificed by CO_2 asphyxiation. Blood was collected from the abdominal aorta and after centrifugation the plasma was stored at -70^{o}C. The small intestine, caecum and colon were removed and opened along the longitudinal axis and rinsed with ice-cold saline. The small intestine was divided into five sections of equal length. The caecum and colon were separated from the small intestine and kept together for analysis. The intestinal sections were spread flat on microscope slides. Each section of the intestine and colon and caecum was analyzed under a stereomicroscope attached to a monitor. The number and diameter of each adenoma was recorded for all intestinal sections separately. The observers keeping record were blinded to the treatment. The intestinal adenomas were excised from the tissue and the normal-appearing mucosa that was left behind was scraped off from lamina propria. The tissue samples were snap frozen in liquid nitrogen and stored at -70^{o}C. For immunostaining analyses, samples were collected from the distal small intestine, fixated in buffered 4% paraformaldehyde and processed for paraffin

sections. For microarray analysis, another 0.5 cm section was collected from the same intestinal area and stored in RNA later solution (Qiagen) at -20 ^{o}C.

Immunostaining

Paraffin tissue sections were deparaffinised and subjected to heat-induced antigen retrieval (microwave heating for 15 min at 700W power in 250 ml of buffer, followed by a 20 min cooling period). Automated immunostaining was performed using the LabVision Autostainer 480 and the Ultravision detection system (LabVision, Thermo Fisher Scientific). Proliferating cells were identified with an antibody against Ki67 antigen (clone SP6, Labvision), mitotic cells with anti-phospho-histone H3 (#06-570, Millipore), apoptotic cells with an antibody against cleaved caspase 3 (#CP229, Biocare), T lymphocytes with anti-CD3ε (clone SP7, Neomarkers), regulatory T cells with anti-FoxP3 (clone FJK16s, eBioscience) and B lymphocytes with anti-CD45R (clone RA3-6B2, Invitrogen). Antigen retrieval was performed using Na-citrate buffer, pH 6, for all markers except for cleaved caspase 3, where Tris-HCl-EDTA, pH8 was used. The immunostained sections were photographed using a Leica DM4000 microscope and an Olympus DP70 camera. The digital photomicrographs were analysed using ImageJ.

Western blotting

Samples were prepared as described previously (21). Briefly, proteins were isolated from morphologically normal mucosa of the distal small intestine, representing approximately 40% of the total small intestine. For proteinase and phosphatase inhibition, 0.4 mM leupeptin, 3.0 μM pepstatin and 1.0 mM PMSF (in DMSO), 0.5 M NaF and Na_3VO_4 were

added to the homogenisation buffer (20 mM Tris-HCl, pH 7.4; 2 mM EDTA; 10 mM EGTA; 0.25 M saccharose). For the whole mucosa lysate, 10% triton-x was added to the homogenate, after which the sample was mixed for 20 minutes with 5 minutes intervals, followed by centrifugation (15 000 x g 10 minutes at 4^{o}C). All protein samples were stored at -70^{o}C. Protein samples were loaded in equal concentrations to SDS-PAGE gels (6.5% gels for beta-catenin and AKT/phospho AKT, 10% gels for others). All samples were analyzed at least as duplicates. An internal standard was used in each gel to control interassay variation. After electrophoresis the proteins were transferred to either nitrocellulose (Hybond ECL membrane, Amersham Pharmacia Biotech.) or PVDF (Hybond P membrane, Amersham Pharmacia Biotech.) membrane. Membranes were incubated overnight in blocking solution containing 3.5% non-fat soya (β-catenin and lamin B analysis) or 5% non-fat milk (other analyses) in Tris-buffered saline with 0.1% Tween. Membranes were incubated with primary antibodies for 2 hours or overnight with phospho-specific antibodies. Primary antibodies were anti-β-catenin (sc-7199, Santa Cruz Biotechnology), anti-phospho-β-catenin (Ser552 #9566 and Ser675 #4176, Cell Signaling Technology), anti-ERK1 (sc-94, Santa Cruz Biotechnology), anti-phospho-p44/42 (#9101, Cell Signaling Technology), anti-AKT (#9272, Cell Signaling Technology), anti-phospho-AKT (#9271, Cell Signaling Technology), anti-S6 (#2217, Cell Signaling Technology), anti-phospho-S6 (#4858, Cell Signaling Technology), anti-PDK4 (NBP1-07047, Novus Biologicals), anti-lamin B (sc-6216, Santa Cruz Biotechnology), and anti-β-actin (A541, Sigma). For protein detection, secondary antibodies (sc-2030 and sc-2031, Santa Cruz Biotechnology) and enhanced chemiluminescence reagents ECL or ECL+ (GE Healthcare) were used. The levels of phosphorylated and total protein were analyzed using the same membrane. After incubating the membrane with a phospho-specific antibody, the membrane was stripped in stripping buffer (78 mM Tris-HCl, 2% SDS, 0.68%

(V/V) mercaptoethanol) for 20 minutes at 65^{o}C, followed by incubation in TBS-Tween for 20 minutes at 65^{o}C and incubation in TBS-Tween for 20 minutes at room temperature. Blots were transferred to X-ray film (Amersham) and scanned and analyzed by GSA-800 Calibrated Imaging Densitometer and Quantity One Program (BioRad Laboratories). β-actin and lamin B were used to control equal loading of protein samples. Phosphorylated forms of β-catenin and PDK4 were detected using Odyssey infrared imager as described by Marttinen et al. (21).

DNA isolation and analysis of loss-of-heterozygosity by qPCR

Genomic DNA was extracted from histologically normal mucosa of the distal small intestine using the DNeasy Blood & Tissue Kit (Qiagen, Valencia, CA).

The relative copy numbers of *Min* and wild-type *Apc* alleles in these genomic DNA samples were quantified by multiplex quantitative PCR, using the following primers and allelic discrimination probes: forward primer, 5'-GACAGTTCTCGTTCTGAG-3'; reverse primer, 5'-GTTGGATGGTAAGCACTG-3'; wild-type probe, 5'-[FAM] ctctcTccAaaCttCtgt [BHQ1]-3'; *Min* probe, 5'-[CY3] ctctcTccTaaCttCtgt [BHQ2]-3'. Locked nucleic acid (LNA) nucleotides were used in the probes to increase specificity and are indicated in the probe sequences in capital letters. The LNA probes were designed and synthesized by Sigma Aldrich. The amplification was carried out using the Maxima Probe qPCR Master Mix (Life Technologies) and a Stratagene MX3005P qPCR instrument (Agilent Technologies). The cycling conditions were: an initial denaturation at 95°C for 15 min, followed by 40 cycles of 95°C for 10 s and 61°C for 30 s.

To obtain the actual ratio of *Min* and wild-type sequences in each sample, fold changes relative to reference DNA samples from *Min/+* and wild-type mice were first calculated for the *Min* and wild-type probes, respectively. The ratio of these values was then compared to a standard curve obtained from known dilutions of *Min/+* and wild-type DNA. The final results are averages of three separate parallel qPCR experiments. Individual measurements deviating more than 25% from the average of the three parallel runs were excluded from subsequent analyses (6% of all measurements).

RNA isolation and gene expression analyses

Total RNA was extracted from histologically normal-appearing mucosa of the distal small intestine using the RNeasy Mini kit (Qiagen). RNA was quantified using the Nanodrop 1000 spectrophotometer (Thermo Scientific), and the integrity of the RNA samples was verified using Bioanalyzer 2100 (v2.6, Agilent Technologies, Inc.). Equal amounts of total RNA was taken from each mouse to make 8 pooled samples (2 samples per diet and per sex, containing 1-3 mice per sample). The quality of the pooled RNA samples was again controlled by Bioanalyzer (RIN >8). The pooled samples were then analyzed by Agilent Whole Mouse Genome 4x44K microarray assay. The labeling, hybridization and scanning were performed at the Biomedicum Functional Genomics Unit, University of Helsinki.

Statistical analysis

The non-parametric Mann-Whitney U-test was used to compare the data between the groups. The associations between variables were analyzed with the non-parametric Spearman's correlation test. All statistical analyses were performed using the PASW Statistic

18 for Windows software (SPSS Inc.). The p-value of P< 0.1 was conceded as a significant difference between the groups from Western blot analyses.

The gene-expression microarray data was analyzed with the CSC Chipster v1.4.6 software (http://chipster.csc.fi/). The data was normalized using mean normalization, and genes with detectable expression in four chips were used in further analyses. Genes with changes ±1.2 and $P < 0.05$ were considered differentially expressed. The functional enrichment analyses were conducted with DAVID (22, 23). The data sets were reviewed and passed the following quality controls: The lists contained many important genes as expected for the study, the number of genes was reasonable, in range of few hundred genes in each list, the genes passed statistical thresholds (FC 1.2, $P<0.05$) so that the threshold would not have to be sacrificed (e.g., fold changes ≥1.1 and P-value ≤0.2) to reach a comfortable gene size, and notable portion of up- or down-regulated genes were involved in certain interesting biological processes, such as energy metabolism and Wnt signaling. The lists of enriched functional pathways were compared between the lists. The analysis of large gene lists is an exploratory, computational procedure rather than a purely statistical method. In order to diminish the effect of false positives, as only a large body of genes with similar functions may show a significant result in the enrichment analysis, statistics were applied to detect enriched functional categories or pathways associated with the genes regulated by the WD feed, using Database for Annotation, Visualization and Integrated Discovery (DAVID) v6.7 (23).

Results

Adenoma formation and loss of heterozygosity (LOH) of the *Apc* gene was increased in *Min/+* mice consuming WD

The average number of adenomas in the total small intestine was two times higher in the Western-type diet (WD) mice (median 36; range 14-76) compared to the control mice (Fig. 1A; median 18; range 7-38; $P = 0.003$). Colon or caecum adenomas were rare and there was no difference between the groups. The average size of the adenomas did not differ between the groups (Fig. 1B; $P = 0.781$). Neither was there any difference in the weight gain between the diet groups.

Loss of *APC* heterozygosity was analyzed by allele-specific quantitative PCR in genomic DNA isolated from tissue samples from the distal part of the small intestine. The ratio of the *Min* allele to the wild-type allele was significantly higher in the WD mice (Fig.1C; $P = 0.026$), suggesting that the high risk WD accelerated LOH. LOH was associated with adenoma number in the total small intestine (Fig. 1D; $r_s = 0.573$, $P = 0.03$).

Mucosal β-catenin, proliferation and apoptosis were not changed in the WD mice

Levels of total β-catenin were analyzed from whole mucosa lysate and were 7.85 (median, min 2.48 max 14.6) in the WD mice compared to 5.54 (median, min 0.58, max 11.93) in the control group. The difference, however, was not significant ($P = 0.118$). The Ser552 and Ser675 -phospho-β-catenin in nuclear fractions were also measured. The Ser552-phospho-β-

catenin showed a similar non-significant trend for increased nuclear accumulation, as did the total β-catenin (data not shown).

Epithelial proliferation was assessed in the mucosa by the average height of the Ki67 antigen positive zone, measured from the crypt bases, and by the number of mitotic (phospho-histone H3 positive) cells per crypt zone mm^2. The rate of apoptosis was measured by counting cleaved caspase 3 positive cells per mucosa mm^2. Proliferation and apoptosis did not differ between the groups (Fig. 2A and B). However, the ratio of proliferation to apoptosis was slightly lower in the WD mice compared to the controls (Fig 2C. *P* = 0.098).

Decrease in the relative activation of mucosal ERK1/2 and AKT pathways in the WD mice

Phosphorylation of ERK1/2 and AKT were analyzed from whole mucosa lysate from the distal part of the intestine. The activation of the ERK pathway was significantly suppressed in the WD mice. This was seen in both ERK1 (p44) and ERK2 (p42) phosphoprotein levels (*P* = 0.036 and 0.031). When the p42 and p44 protein bands were analyzed together, the relation of phosphorylated to total ERK in the WD mice was 1.07 (min 0.07, max 2.82) while it was 3.38 (min 0.14, max 10.58) in the control mice (Fig. 3A, *P* = 0.045). No difference was seen in the total amount of ERK1 or ERK2 (*P* = 0.43 and *P* = 0.59, respectively). The ratio of phosphorylated AKT to total AKT showed a tendency to decrease in the WD group (Fig. 3B, *P* = 0.090).

Decrease in the relative activation of mucosal mTOR pathway, with increase in PDK4 protein level in the WD mice

The WD mice had a reduced activation of the mTOR pathway as measured in pS6/total S6 levels (medians 0.40 vs. 0.11) (Fig. 3C, $P = 0.057$). No difference was seen in the total amount of S6 between the groups ($P = 0.92$). The microarray data showed an expression level of PDK4 that was nine times higher in the WD mice when compared to the controls. Thus, the protein levels for PDK4 were also measured. These were 13.3 and 10.9 (medians, $P = 0.057$) for WD and control diet respectively (Fig. 3D), confirming an upregulation of PDK4 signaling in the WD mice.

The density of intraepithelial T lymphocytes and mucosal regulatory T cells were higher in the WD mice

The density of intraepithelial $CD3\varepsilon^+$ T lymphocytes and the density of mucosal $FoxP3^+$ regulatory T cells were significantly higher in the WD mice, while the density of mucosal $CD45R^+$ B lymphocytes did not differ significantly between the diet groups (Fig 4A-C; $P = 0.016$, 0.027, 0.129, respectively). Adenoma numbers correlated significantly with the density of $FoxP3^+$ cells (Fig. 4D; $P = 0.006$) and inversely with the density of $CD45R^+$ cells (Fig. 4E; $P = 0.011$).

Global gene expression analyses revealed several changes in the WD mice

Global gene expression profiles in the morphologically normal intestinal mucosa were analyzed using Agilent Mouse Genome 4 x 44K oligonucleotide arrays. To gain further

insight into the diet-induced changes in gene expression, the data were analyzed for enriched pathways and categories. The enriched KEGG and Gene Ontology pathways are listed in Tables 2 and 3.

Based on the enrichment analyses, the WD strongly affected energy metabolism in the intestinal mucosa: the KEGG pathways, starch and sucrose metabolism, pyruvate metabolism, glycolysis/gluconeogenesis and PPAR signaling were significantly different between the groups ($P < 0.05$). The Gene Ontology analysis showed that several genes associated with oxidation/reduction and fatty acid, hexose, glucose and monosaccharide metabolic processes were significantly differently expressed between the control and the WD groups. Of individual genes, the largest difference between groups was found in the expression of PDK4 that was nine times higher in the WD mice when compared to the controls. Other significantly up-regulated genes related to glucose metabolism were glucose-6-phosphatase and glucosidase, while the expressions of TCA-cycle enzyme oxoglutarate dehydrogenase and glycerol phosphate dehydrogenase from oxidative phosphorylation were downregulated in the WD mice.

The genes up-regulated in WD mice and related to fatty acid oxidation and oxidative stress response included several cytochromes, the acyl-CoA thioesterase *Acot12*, the acyl-coenzyme A dehydrogenase *Acadl,* glutathione and thiol reductases, and vanin-1, a sensor of oxidative stress in epithelial cells. The WD had an impact on the regulation of apoptosis and cellular death in the intestinal mucosa by modifying the expression of both pro- and anti-apoptotic genes, including e.g. up-regulation of angiopoietin-like 4 (*Angptl4*) and the

stem cell marker *Bmi1*. The WD also affected the Wnt receptor signaling pathway (as defined by both KEGG and GO). Down-regulation of *Tcf4* (reported with two probes) suggests that Wnt signaling was generally suppressed in the mice consuming WD. Interestingly, GO-based analyses revealed that the tissue organization pathway defined by e.g. filopodium and microspike assembly, as well as cell projection assembly genes, were different between the groups (Table 3).

Discussion

We studied how a high-risk Western diet affects the development of intestinal cancer in a murine model with genetic predisposition to tumorigenesis, the *Min/+* mice. The Western type diet is expected to induce a metabolic stress due to the high fat content and the low content of fiber and several micronutrients. The WD accelerated the initiation of adenomas in our study, but did not promote tumor growth, indicating that the diet primarily impacted the preneoplastic, histologically normal intestinal epithelium.

In the *Min/+* mouse as in the vast majority of human CRC cases the driving force for tumorigenesis is an activation of the Wnt pathway due to the mutation in *Apc* gene. A prerequisite for adenoma formation is loss of *Apc* heterozygosity (LOH) (5). We found an increase in the ratio of the *Min* allele to the wild-type allele in the histologically normal intestinal mucosa in *Min/+* mice consuming WD. This indicates acceleration of LOH by the diet. Furthermore, the LOH results correlated with the numbers of adenomas.

LOH occurs primarily by homologous somatic recombination in both human and *Min/+* adenomas (24). Thus, the increased adenoma formation in WD mice could be partially explained by factors that induce recombination, such as oxidative DNA damage (25, 26). The oxidative stress induced by increased fatty acid metabolism on a high-fat diet has been reported to increase mitochondrial as well as nuclear DNA damage (27, 28). In our WD mice, gene expression analysis showed strongly upregulated oxidation/reduction pathways as well as oxidative stress responses in the intestinal mucosa, compatible with previous observations in the colonic mucosa of WD-fed wild-type mice (29). Oxidative DNA damage can also be caused by inflammation (30). We observed an impact of the WD on the inflammatory status of the intestinal mucosa. The density of intraepithelial $CD3\varepsilon^+$ T lymphocytes and of $FoxP3^+$ regulatory T cells was higher and the density of B lymphocytes lower in the histologically normal mucosa of the WD mice. Akeus et al. (31) found an accumulation of $FoxP3^+$ regulatory T cells and decreased density of B cells in the adenoma tissue of the *Min/+* mouse in comparison to wild-type mouse mucosa, indicating that the immunological balance in the mucosa of our WD mice had already shifted towards the adenoma state.

Our diet was low in calcium and vitamin D, both needed for tight junction physiology. In the calbindin-null mice, a calcium and vitamin D deficient diet resulted in down-regulation of tight junction genes (32). Tight junction protein expression is regulated through ERK1/2 and AKT signaling (33, 34), both of which were clearly down-regulated in our WD mice. Our results suggest that low levels of calcium and vitamin D in the diet negatively affect the expression of tight junction proteins and, as a result, down-regulate the ERK1/2 and AKT

signaling in the WD mice. The microarray expression data showed down-regulation of five tight junction genes, casein kinase 2α1, membrane associated guanylate kinase, PKCδ, spectrinβ2, and symplekin in the WD mice (data not shown). Downregulation of these genes has been shown to promote tumorigenesis in different cancers (35-39). Disruption of the tight junction barrier may also explain the inflammatory changes we observed (40). In addition, differently expressed tissue organization pathways, filopodium, microspike and cell projection assemblies support disturbed tissue or cellular functions in the WD group. Our results are well in line with an earlier study showing that adding calcium and vitamin D significantly decreased the number of colonic tumors in a long-term WD feeding experiment with wild-type mice (3). In this study, folate did not explain tumor formation. As the folate level was the same as in our WD diet, the low folate content probably had no major role for adenoma formation in our study either.

The gene expression data and protein-level analyses show that the WD had a profound effect on energy metabolism in the intestinal mucosa. PDK4 expression was up-regulated at mRNA and protein levels in the WD mice. Together with the activated glucose and fatty acid metabolic pathways, these findings suggest that the WD pushed the intestinal mucosa towards Warburg-type aerobic glycolysis. A switch toward oxidative glycolysis, directly driven by PDKs, is an early step in cellular transformation. Shifting to oxidative glycolysis enables the cancer cells to acquire building blocks for the proliferation of new cells instead of efficient ATP production (8). Glycolysis genes are ubiquitously overexpressed in cancers (41). Thus, the glycolytic switch could pre-program the intestinal epithelium to a carcinogenesis-compatible metabolic state. In mice consuming a WD, PDK4 may be activated

by the high concentrations of free fatty acids, enhanced fatty acid metabolism and up-regulated PPAR signaling, all of which are known to affect PDK expression (42, 43). The decreased Erk signaling is also expected to allow up-regulation of PDK4 expression (13).

Like the ERK1/2 pathway, also the mTOR signaling was clearly down-regulated. mTOR negatively regulates stem cell proliferation and renewal in the intestinal crypts (44). Deregulated ribosomal S6K has been linked to disturbed establishment of a stem/progenitor population (45). It has also been linked to inhibition of mTOR signalling in cancer cell lines with the up-regulated stem cell marker CD133 (46). Our microarray data suggest that the stem cell marker *Bmi1* was up-regulated in the WD mice. The decreased mTOR signaling may also suggest that the high fat diet suppressed insulin signaling in the intestinal epithelium, as observed in other tissues of diet-induced obese mice (47, 48). The potential depression of insulin signaling in the intestinal epithelium may contribute also to the increased PDK4 levels, as observed during starvation and in diabetes (14).

Epithelial proliferation and apoptosis were not markedly changed in WD mice, although the ratio of proliferation to apoptosis showed a tendency ($P = 0.098$) to be lower. However, gene expression analysis showed a clear impact of the WD on both pro- and antiapoptotic pathways in the mucosa, suggesting a disturbance in the regulation of epithelial renewal. The proliferation/apoptosis ratio did not correlate with the number of adenomas, suggesting that the regulation of apoptosis as such is not the direct cause for increased adenoma number.

Mucosal β-catenin levels showed only a tendency towards elevation in the WD mice, and the gene expression data suggest that the Wnt pathway was rather attenuated than activated. This suggests that other functions of truncation of *Apc* in the WD mice, beside changes in β-catenin-regulated transcription, may explain the higher number of polyps. The location of a mutation in the *Apc* gene regulates the number of adenomas and the level of β-catenin in epithelial tissue (49). In comparison with the *Min* mutation, an Apc^{1322T} mutation results in lower β-catenin levels in the enterocytes but a much higher total number of polyps (49). In our earlier study in the *Min/+* mouse, β-catenin levels in adenomas were significantly associated with adenoma size but not number, demonstrating the active role of β-catenin in driving the growth of tumor tissue rather than promoting the initiation phase (50).

All in all, our results suggest that a high-risk Western diet that is high in fat and low in calcium and vitamin D, primes the intestinal epithelium to tumorigenesis by changing tissue organization and programming a cancer-type energy metabolism together with induced oxidative stress, which accelerates the loss of *Apc* heterozygosity. The synergistic effects of the genetic predisposition and the diet result in significantly accelerated intestinal tumorigenesis.

References

1. Baltgalvis KA, Berger FG, Pena MM, Davis JM, Carson JA. The interaction of a high-fat diet and regular moderate intensity exercise on intestinal polyp development in ApcMin/+ mice. Cancer Prev Res 2009;2:641-9.

2. Newmark HL, Yang K, Lipkin M, Kopelovich L, Liu Y, Fan K, et al. A Western-style diet induces benign and malignant neoplasms in the colon of normal C57Bl/6 mice. Carcinogenesis 2001;22:1871-5.

3. Newmark HL, Yang K, Kurihara N, Fan K, Augenlicht LH, Lipkin M. Western-style diet-induced colonic tumors and their modulation by calcium and vitamin D in C57Bl/6 mice: a preclinical model for human sporadic colon cancer. Carcinogenesis 2009;30:88-92.

4. Yang K, Kurihara N, Fan K, Newmark H, Rigas B, Bancroft L, et al. Dietary induction of colonic tumors in a mouse model of sporadic colon cancer. Cancer Res 2008;68:7803-10.

5. Powell SM, Zilz N, Beazer-Barclay Y, Bryan TM, Hamilton SR, Thibodeau SN, et al. APC mutations occur early during colorectal tumorigenesis. Nature 1992;359:235-7

6. Boivin GP, Washington K, Yang K, Ward JM, Pretlow TP, Russell R, et al. Pathology of mouse models of intestinal cancer: consensus report and recommendations. Gastroenterology 2003;124:762-77.

7. Pate KT, Stringari C, Sprowl-Tanio S, Wang K, TeSlaa T, Hoverter NP, et al. Wnt signaling directs a metabolic program of glycolysis and angiogenesis in colon cancer. EMBO J 2014;33:1454-73.

8. Heiden MGV, Cantley LC, Thompson CB. Understanding the Warburg effect: the metabolic requirements of cell proliferation. Science 2009;324:1029-33.

9. Weinberg F, Hamanaka R, Wheaton WW, Weinberg S, Joseph J, Lopez M, et al. Mitochondrial metabolism and ROS generation are essential for Kras-mediated tumorigenicity. PNAS 2010;107:8788-93.

10. Hsu PP, Sabatini DM. Cancer cell metabolism: Warburg and beyond. Cell 2008;134:703-7.

11. Leclerc D, Lévesque N, Cao Y, Deng L, Wu Q, Powell J, et al. Genes with aberrant expression in murine preneoplastic intestine show epigenetic and expression changes in normal mucosa of colon cancer patients. Cancer Prev Res 2013;6:1171-81.

12. Michelakis ED, Webster L, Mackey JR. Dichloroacetate (DCA) as a potential metabolic-targeting therapy for cancer. Br J Cancer 2008;99:989-94.

13. Grassian AR, Metallo CM, Coloff JL, Stephanopoulos G, Brugge JS. Erk regulation of pyruvate dehydrogenase flux through PDK4 modulates cell proliferation. Genes Dev 2011;25:1716-33.

14. Jeong JY, Jeoung NH, Park KG, Lee IK. Transcriptional regulation of pyruvate dehydrogenase kinase. Diabetes Metab J 2012;36:328-35.

15. Deschênes-Simard X, Kottakis F, Meloche S, Ferbeyre G. ERKs in cancer: friends or foes? Cancer Res 2014;74:412-9.

16. Hales EC, Taub JW, Matherly LH. New insights into Notch1 regulation of the PI3K-AKT-mTOR1 signaling axis: targeted therapy of γ-secretase inhibitor resistant T-cell acute lymphoblastic leukemia. Cell Signal 2014;26:149-61.

17. Mutanen M, Pajari AM, Oikarinen SI. Beef induces and rye bran prevents the formation of intestinal polyps in Apc(Min) mice: relation to beta-catenin and PKC isozymes. Carcinogenesis 2000;21:1167-73.

18. MacFarlane AJ, Perry CA, McEntee MF, Lin DM, Stover PJ. Mthfd1 is a modifier of chemically induced intestinal carcinogenesis. Carcinogenesis 2011;32:427-33.

19. Ju J, Kwak Y, Hao X, Yang CS. Inhibitory effects of calcium against intestinal cancer in human colon cancer cells and Apc(Min/+) mice. Nutr Res Pract 2012;6:396-404.

20. Zheng W, Wong KE, Zhang Z, Dougherty U, Mustafi R, Kong J, et al. Inactivation of the vitamin D receptor in APC(min/+) mice reveals a critical role for the vitamin D receptor in intestinal tumor growth. Int J Cancer 2012;130:10-9.

21. Marttinen M, Päivärinta E, Storvik M, Huikko L, Luoma-Halkola H, Piironen V, et al. Plant stanols induce intestinal tumor formation by up-regulating Wnt and EGFR signaling in Apc Min mice. J Nutr Biochem 2013;24:343-52.

22. Dennis G Jr, Sherman BT, Hosack DA, Yang J, Gao W, Lane HC, et al. DAVID: Database for Annotation, Visualization, and Integrated Discovery. Genome Biol 2003;4:P3.

23. Huang da W, Sherman BT, Lempicki RA. Systematic and integrative analysis of large gene lists using DAVID bioinformatics resources. Nat Protoc 2009;4:44-57.

24. Haigis KM, Caya JG, Reichelderfer M, Dove WF. Intestinal adenomas can develop with a stable karyotype and stable microsatellites. PNAS 2002;99:8927-31.

25. Rani V, Neumann CA, Shao C, Tischfield JA. Prdx1 deficiency in mice promotes tissue specific loss of heterozygosity mediated by deficiency in DNA repair and increased oxidative stress. Mutat Res 2012;735:39-45.

26. Turner DR, Dreimanis M, Holt D, Firgaira FA, Morley AA. Mitotic recombination is an important mutational event following oxidative damage. Mutat Res 2003;522:21-6.

27. De Assis AM, Rieger DK, Longoni A, Battu C, Raymundi S, da Rocha RF, et al. High fat and highly thermolyzed fat diets promote insulin resistance and increase DNA damage in rats. Exp Biol Med 2009;234:1296-304.

28. Yuzefovych LV, Musiyenko SI, Wilson GL, Rachek LI. Mitochondrial DNA damage and dysfunction, and oxidative stress are associated with endoplasmic reticulum stress, protein degradation and apoptosis in high fat diet-induced insulin resistance mice. PLoS ONE 2013;8:e54059.

29. Erdelyi I, Levenkova N, Lin EY, Pinto JT, Lipkin M, Quimby FW, et al. Western-style diets induce oxidative stress and dysregulate immune responses in the colon in a mouse model of sporadic colon cancer. J Nutr 2009;139:2072-8.

30. Meira LB, Bugni JM, Green SL, Lee CW, Pang B, Borenshtein D, et al. DNA damage induced by chronic inflammation contributes to colon carcinogenesis in mice. J Clin Invest 2008;118:2516-25.

31. Akeus P, Langenes V, von Mentzer A, Yrlid U, Sjöling Å, Saksena P, et al. Altered chemokine production and accumulation of regulatory T cells in intestinal adenomas of APC(Min/+) mice. Cancer Immunol Immunother 2014;63:807-19.

32. Hwang I, Yang H, Kang HS, Ahn C, Hong EJ, An BS, et al. Alteration of tight junction gene expression by calcium- and vitamin D-deficient diet in the duodenum of calbindin-null mice. Int J Mol Sci 2013;14:22997-3010.

33. Lin N, Xu LF, Sun M. The protective effect of trefoil factor 3 on the intestinal tight junction barrier is mediated by toll-like receptor 2 via a PI3K/Akt dependent mechanism. Biochem Biophys Res Commun 2013;440:143-9.

34. Seo GS, Jiang WY, Park PH, Sohn DH, Cheon JH, Lee SH. Hirsutenone reduces deterioration of tight junction proteins through EGFR/Akt and ERK1/2 pathway both converging to HO-1 induction. Biochem Pharmacol 2014;90:115-25.

35. Chang H, Zhang C, Cao Y. Expression and distribution of symplekin regulates the assembly and function of the epithelial tight junction. Histochem Cell Biol 2012;137:319-27.

36. Feng X, Jia S, Martin TA, Jiang WG. Regulation and involvement in cancer and pathological conditions of MAGI1, a tight junction protein. Anticancer Res 2014;34:3251-6.

37. Hernández-Maqueda JG, Luna-Ulloa LB, Santoyo-Ramos P, Castañeda-Patlán MC, Robles-Flores M. Protein kinase C delta negatively modulates canonical Wnt pathway and cell proliferation in colon tumor cell lines. PLoS One 2013;8:e58540.

38. So KS, Rho JK, Choi YJ, Kim SY, Choi CM, Chun YJ, et al. Akt/mTor down-regulation by CX-4945, a CK2 inhibitor, promotes apoptosis in chemorefractory non-small cell lung cancer cells. Anticancer Res 2015;35:1537-42.

39. Zhi X, Lin L, Yang S, Bhuvaneshwar K, Wang H, Gusev Y, et al. βII-Spectrin (SPTBN1) suppresses progression of hepatocellular carcinoma and Wnt signaling by regulation of Wnt inhibitor kallistatin. Hepatol 2015;61:598-612

40. Lee SH. Intestinal permeability regulation by tight junction: implication on inflammatory bowel diseases. Intest Res 2015;13:11-8.

41. Altenberg B, Greulich KO. Genes of glycolysis are ubiquitously overexpressed in 24 cancer classes. Genomics 2004;84:1014-20.

42. Huang B, Wu P, Bowker-Kinley MM, Harris RA. Regulation of pyruvate dehydrogenase kinase expression by peroxisome proliferator-activated receptor-alpha ligands, glucocorticoids, and insulin. Diabetes 2002;51:276-83.

43. Zhang L, Mori J, Wagg C, Lopaschuk GD. Activating cardiac E2F1 induces up-regulation of pyruvate dehydrogenase kinase 4 in mice on a short term of high fat feeding. FEBS Lett 2012;586:996-1003.

44. Yilmaz ÖH, Katajisto P, Lamming DW, Gültekin Y, Bauer-Rowe KE, Sengupta S, et al. mTORC1 in the Paneth cell niche couples intestinal stem-cell function to calorie intake. Nature 2012;486:490-5.

45. Korta DZ, Tuck S, Hubbard EJ. S6K links cell fate, cell cycle and nutrient response in C. elegans germline stem/progenitor cells. Development 2012;139:859-70.

46. Matsumoto K, Arao T, Tanaka K, Kaneda H, Kudo K, Fujita Y, et al. mTOR signal and hypoxia-inducible factor-1 alpha regulate CD133 expression in cancer cells. Cancer Res 2009;69:7160-4.

47. Katta A, Kundla S, Kakarla SK, Wu M, Fannin J, Paturi S, et al. Impaired overload-induced hypertrophy is associated with diminished mTOR signaling in insulin-resistant skeletal muscle of the obese Zucker rat. Am J Physiol Regul Integr Comp Physiol 2010;299:R1666-75.

48. Medeiros C, Frederico MJ, da Luz G, Pauli JR, Silva ASR, Pinho RA, et al. Exercise training reduces insulin resistance and upregulates the mTOR/p70S6k pathway in cardiac muscle of diet-induced obesity rats. J Cell Physiol 2011;226:666-74.

49. Pollard P, Deheragoda M, Segditsas S, Lewis A, Rowan A, Howarth K, et al. The Apc 1322T mouse develops severe polyposis associated with submaximal nuclear beta-catenin expression. Gastroenterology 2009;136:2204-13.

50. Pajari AM, Rajakangas J, Päivärinta E, Kosma VM, Rafter J, Mutanen M. Promotion of intestinal tumor formation by inulin is associated with an accumulation of cytosolic beta-catenin in Min mice. Int J Cancer 2003;106:653-60.

TABLES

Table I: Composition of diets

Component	AIN-93G	Western diet
protein, %kcal	18.8	18.5
CHO, %kcal	63.9	42.3
fat, %kcal	17.2	39.2
milk fat; %fat/ %diet	-	66.4/ 13.2
oil; %fat/ %diet	100/ 7.0	33.6/ 6.7
kcal/g	3.8	4.6
Ca, g/kg	5.0	0.5
folic acid, mg/kg	2.0	0.2
vitamin D, IU/kg	1000	100

Table 2. Enriched KEGG pathways at significance level of $P < 0.05$ (±1.2 fold change) in the WD group as compared to the control group.

KEGG Pathway	Number of genes	P - value
Starch and sucrose metabolism	5	0.0074
Pyruvate metabolism	5	0.0012
Glycolysis/Gluconeogenesis	6	0.0160
PPAR signalling pathway	6	0.0280

Table 3. Enriched GO biological processes the WD group as compared to the control group. Differences were considered significant at $P < 0.05$.

GO pathway	Number of genes	*P* - value
Oxidation reductation	29	0.0004
Filopodium assembly	4	0.0009
Microspike assembly	4	0.0013
Regulation of apoptosis	23	0.0027
Regulation of programmed cell death	23	0.0031
Regulation of cell death	23	0.0034
Fatty acid metabolic process	11	0.0051
Hexose metabolic process	10	0.0088
Glucose metabolic process	9	0.0088
Regulation of transcription from RNA polymerase promoter	23	0.0094
Cell projection assembly	6	0.0150
Transmembrane transport	18	0.0160
Monosaccharide metabolic process	10	0.0180
Wnt receptor signaling pathway	8	0.0190
Regulation of small GTPase mediated signal transduction	11	0.0210
Muscle maintanence	3	0.0210

FIGURE LEGENDS

Figure 1. The high-risk Western-type diet (WD) enhanced intestinal tumorigenesis and loss of *APC* heterozygosity in *Min/+* mice (n = 12-14 per group). A. The mean number of adenomas in the small intestine was increased as compared to the AIN-93G control diet in a 10-week feeding study. B. The diameter of adenomas did not differ. C. The ratio of the *Min* to the wild-type allele was significantly higher in the WD group and (D) correlated with adenoma numbers.

Figure 2. The high-risk Western-type diet (WD) did not change (A) the proliferation or (B) apoptosis indexes in the mucosa of the small intestine in *Min/+* mice (n = 12-14 per group), as compared to the AIN-93G control diet. C. The ratio between proliferation and apoptosis was, however lower on the WD diet. Examples of immunostainings for Ki67 antigen (D) and cleaved caspase 3 (E) are shown below.

Figure 3. The high-risk Western-type diet (WD) induced changes in central pathways involved in carcinogenesis in *Min/+* mice (n = 12-14 per group). The activation of the ERK (A), AKT (B) and mTOR (C) pathways was suppressed in the WD mice as compared to the AIN-93G mice as assessed by the relation of phosphorylated to total protein levels in Western blots. D. WD diet up-regulated PDK4 signaling reflected in higher PDK4 protein levels in the WD group. Representative examples of Western blots are shown below.

Figure 4. The high-risk Western-type diet (WD) changes inflammatory status in the mucosa of *Min/+* mice (n = 12-14 per group). The density of intraepithelial $CD3\varepsilon^+$ T lymphocytes (A) and the density of mucosal $FoxP3^+$ regulatory T cells (B) in the distal small intestine was increased in the WD group. The density of mucosal $CD45R^+$ B lymphocytes did not differ significantly between the diet groups (C). Examples of immunostainings for these markers are shown below the boxplots. The number of adenomas correlated significantly with (*D*) the density of $FoxP3^+$ cells and inversely with (E) the density of $CD45R^+$ cell.

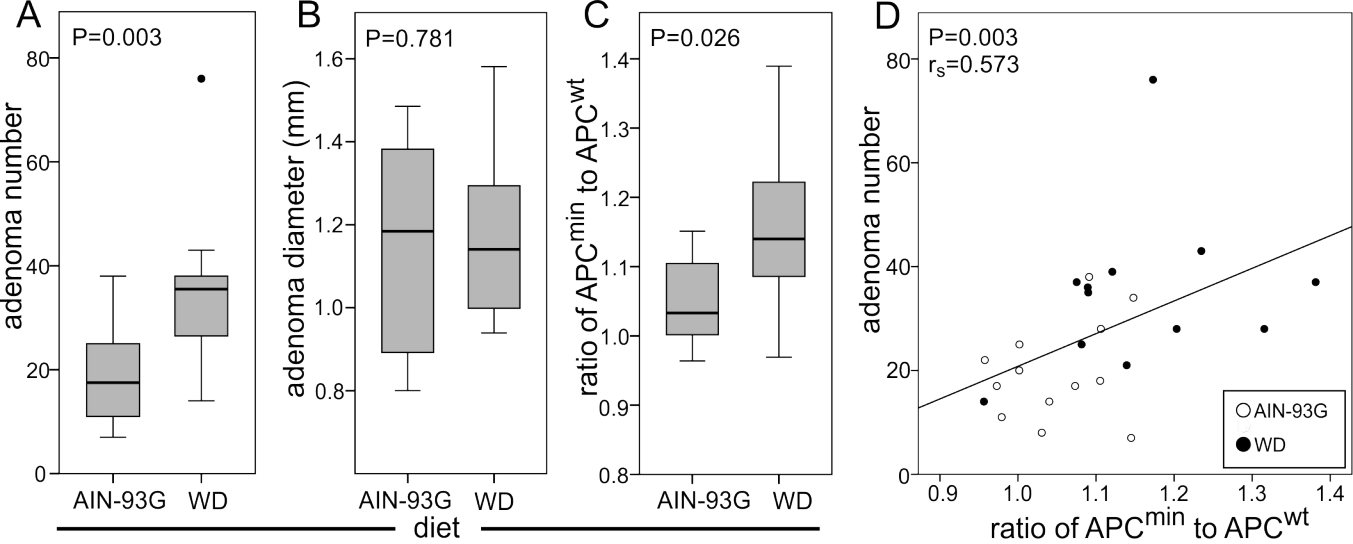
A
P=0.003
adenoma number
80
60
40
20
0
AIN-93G
WD
B
P=0.781
adenoma diameter (mm)
1.6
1.4
1.2
1.0
0.8
AIN-93G
WD
C
P=0.026
ratio of APCmin to APCwt
1.4
1.3
1.2
1.1
1.0
0.9
0.8
AIN-93G
WD
diet
D
P=0.003
rs=0.573
adenoma number
80
60
40
20
0
0.9
1.0
1.1
1.2
1.3
1.4
ratio of APCmin to APCwt
AIN-93G
WD

FIGURE 1

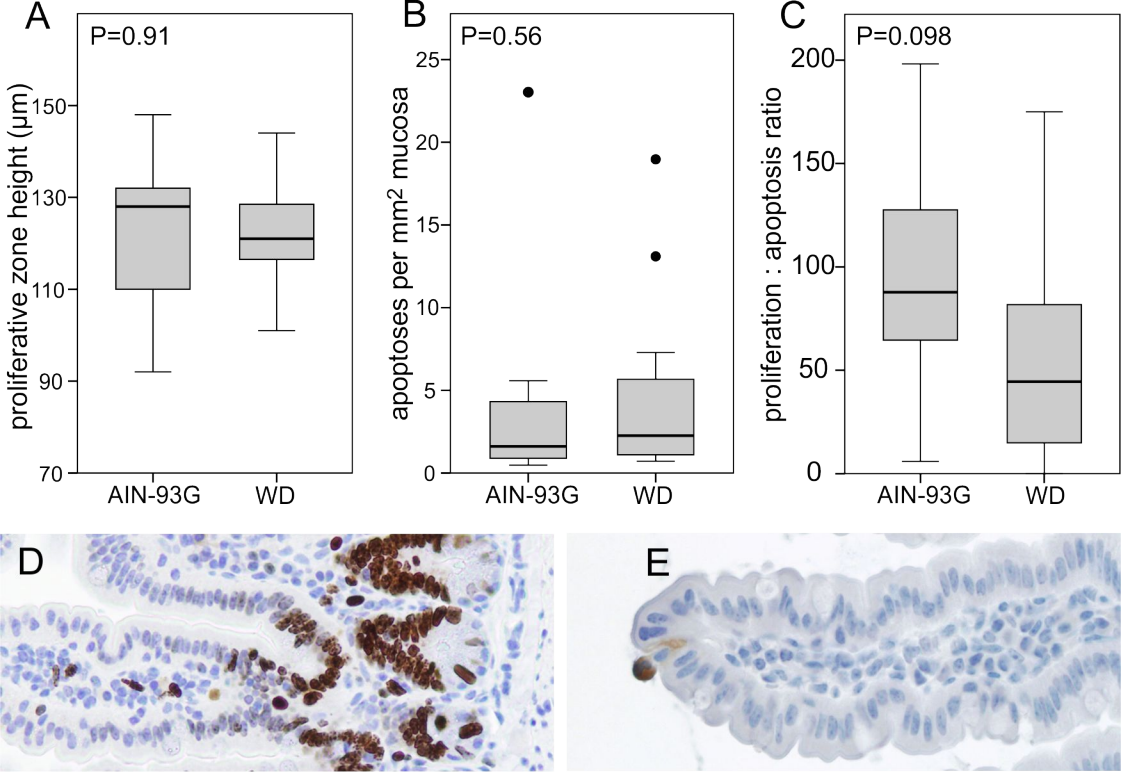
A
P=0.91
proliferative zone height (µm)
150
130
110
90
70
AIN-93G
WD
B
P=0.56
apoptoses per mm2 mucosa
25
20
15
10
5
0
AIN-93G
WD
C
P=0.098
proliferation : apoptosis ratio
200
150
100
50
0
AIN-93G
WD
D
E

FIGURE 2

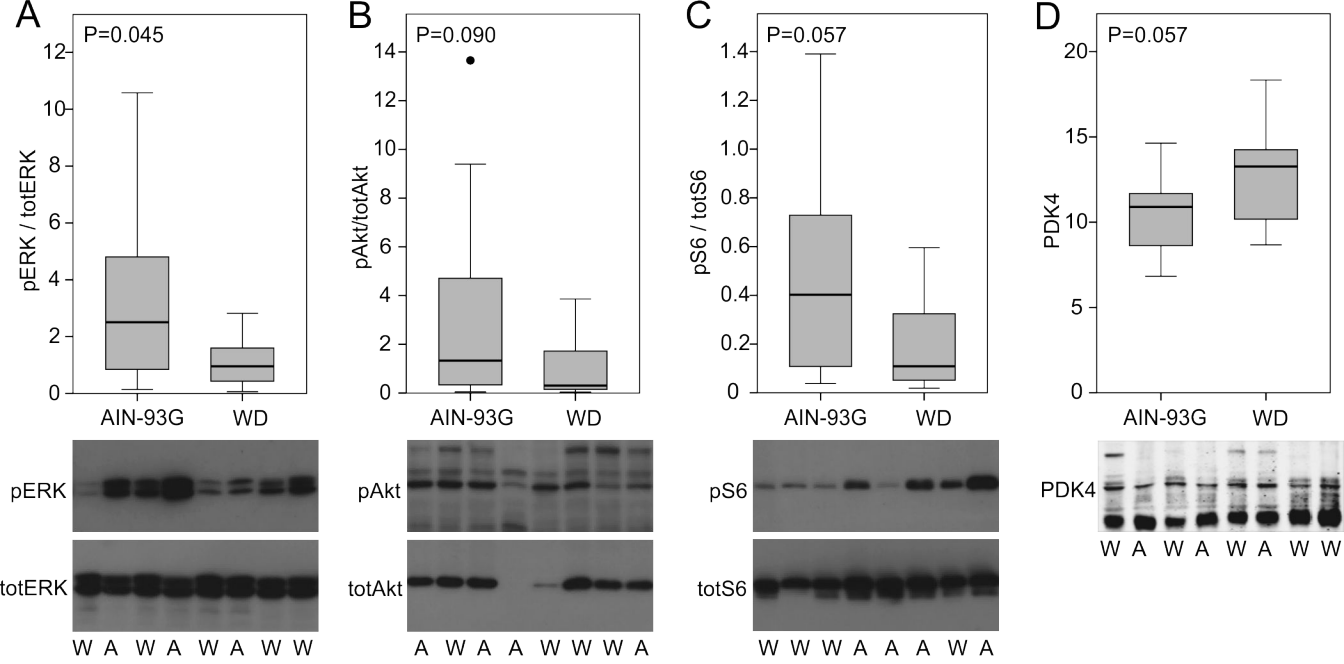
A
P=0.045
pERK / totERK
AIN-93G
WD
pERK
totERK
W A W A W A W W
B
P=0.090
pAkt/totAkt
AIN-93G
WD
pAkt
totAkt
A W A A W W W A
C
P=0.057
pS6 / totS6
AIN-93G
WD
pS6
totS6
W W W A A A W A
D
P=0.057
PDK4
AIN-93G
WD
PDK4
W A W A W A W W

FIGURE 3

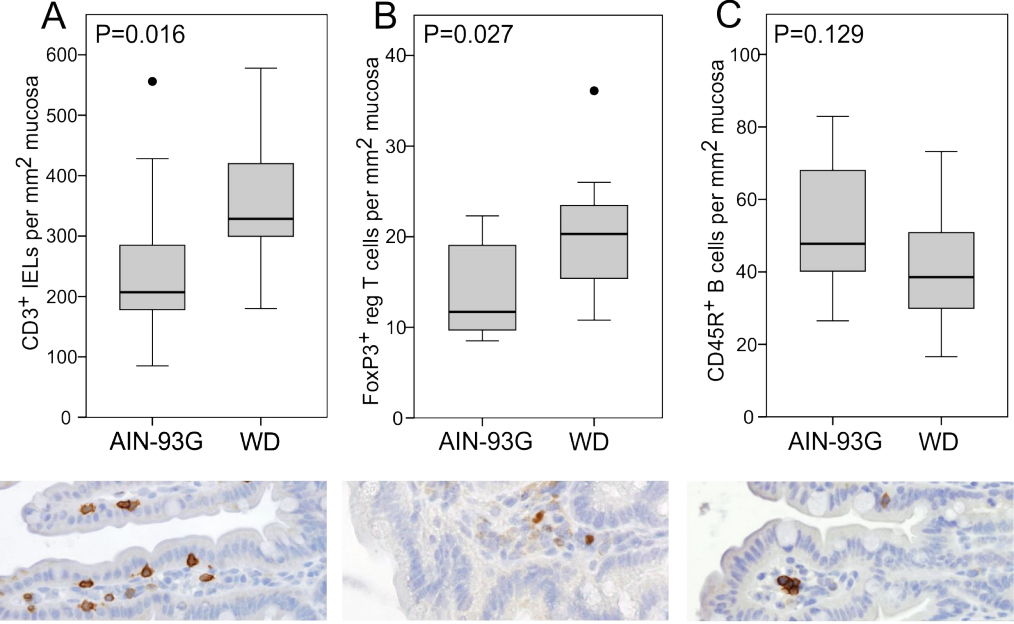
A
P=0.016
CD3+ IELs per mm2 mucosa
600
500
400
300
200
100
0
AIN-93G
WD
B
P=0.027
FoxP3+ reg T cells per mm2 mucosa
40
30
20
10
0
AIN-93G
WD
C
P=0.129
CD45R+ B cells per mm2 mucosa
100
80
60
40
20
0
AIN-93G
WD

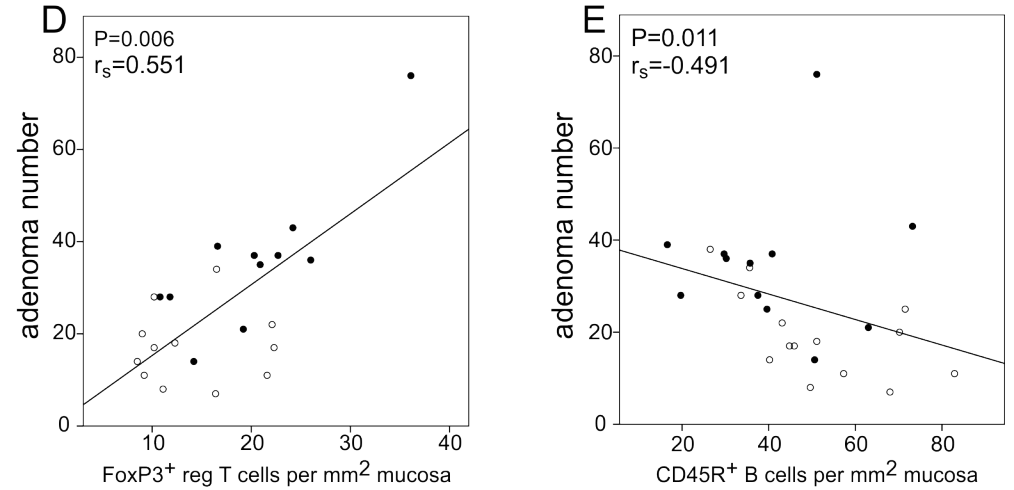
D
P=0.006
rs=0.551
adenoma number
80
60
40
20
0
10
20
30
40
FoxP3+ reg T cells per mm2 mucosa
E
P=0.011
rs=-0.491
adenoma number
80
60
40
20
0
20
40
60
80
CD45R+ B cells per mm2 mucosa

FIGURE 4